Electronic Supplementary Information(ESI)

Non-inertial lift induced migration for label-free sorting of cells in a co-flowing aqueous two-phase system

S. Hazra[1], K. S. Jayaprakash[1], K. Pandian[1], A. Raj[1], S. K. Mitra[2] and A. K. Sen[1,*]

[1]Department of Mechanical Engineering, Indian Institute of Technology Madras, Chennai-600036, India.
[2]Waterloo Institute for Nanotechnology, University of Waterloo, Ontario N2L 3G1, Canada.

[*]Author to whom correspondence should be addressed. Email: ashis@iitm.ac.in

S.1 Materials and Methods

S.1.1 *Measurement of properties*

Dextran (M_r 450,000 – 650,000 , CAS 9004-54-0) powder and poly (ethylene glycol) (PEG) (M_r 35,000, CAS 25322-68-3) flakes were obtained from Sigma-Aldrich, USA. PEG at 10 w/w % was added to 1X filtered PBS and its pH was measured to be 7.25. Dextran was added to 1X PBS at 30 w/w % (pH ~ 6.9) and cell suspension was mixed with it at 1:5 volume ratio, which gives a resultant concentration of dextran as 26 w/w %. Density and viscosities of the aqueous phases were measured using a viscometer (Stabinger Viscometer™, Anton Paar, Austria) and Rheometry was performed using Anton Paar Rheometer MCR 301 and MCR 502. Measurements were repeated five times and average values were taken for further analysis. Density and viscosity of dextran 26 w/w % solution are measured to be 1105.88 kg/m^3 and 0.28331 Pa-s, respectively. Density and viscosity of PEG 10 w/w % solution are measured to be 1020.5 kg/m^3 and 0.02186 Pa-s, respectively. As dextran and PEG combination offers ultralow interfacial tension[1–3], it is challenging to estimate the interfacial tension (IFT) value. Following the pendant drop method described in literature[4], IFT was measured to be 180 µN/m (see section S.1.1.I(b)) which compares well (within 12%) with a value of 160 µN/m estimated using a Droplet Size Analyzer (DSA 25,Krüss GmbH, Germany) (see section S.1.1.I(a)). The latter value was used for further analyses. The measured properties were used in the simulations to determine the velocity and strain rate profiles and for estimating the different forces. Simulations were performed using Ansys 14.0 using Volume of Fluid method in the Fluent module and strain rates for different combinations of flowrates were determined.

S.1.2 *Preparation of cancer cell suspension*

Breast cancer cell lines MDA-MB-231 and MCF-7 were obtained from the National Centre for Cell Science, (NCCS, Pune, India) and grown according to the protocols. Briefly, Leibnovitz L-15 medium was supplemented with 10% Fetal Bovine Serum and Antibiotic antimycotic 100X solution (Himedia, Mumbai, India). The cells were cultured at 37 ℃ in a humid atmosphere containing 5% CO_2. The above two cell lines, being highly metastatic, were used to mimic CTCs. Before the experiments, required number of cells were detached using trypsin EDTA, washed and re-suspended in 50 µl fresh media. The suspended cells were then mixed with dextran.

S.1.3 *Antibody tagging and incubation*

The sorted cells were re-suspended in triple the volume of PBS and cells were collected after centrifugation at 1500 rpm for 10 min. The cell pellet was incubated in blocking buffer for 15 min at room temperature and washed with PBS. For antibody treatment, the pellet was re-suspended in 80 µl of FACS Buffer (PBS supplemented with 1% BSA and 2mM EDTA (pH 7.4) and then mixed with 5µl of direct conjugated EpCAM-PE antibody (BD Biosciences, San Jose, CA, USA) and incubated at 4 °C overnight. After washing with PBS, cell images were captured for further analysis.

S.1.4 *Processing of blood sample*

2 to 4 ml of Sample blood from healthy volunteers was obtained at our institute hospital (IIT Madras, Chennai) after obtaining ethical clearance. Sample blood was collected in vacutainer tubes (BD Biosciences, San Jose, CA, USA) containing EDTA as an anticoagulant. The red blood cells were then lysed using 2 mL Sigma RBC lysis buffer (Roche, Sigma Aldrich, USA) and incubated for 15 min at room temperature. The lysis was followed by PBS washes twice and then PBMCs were collected by centrifugation at 1500 rpm for 10 min. Finally, the sample was re-suspended in 50 µl PBS. The PBMC samples were spiked with the cancer cells just prior to the sorting experiments.

S.1.5 *Antibody tagging and incubation*

After sorting, cells were re-suspended in triple the volume of PBS and collected by centrifugation at 1500 rpm for 10 min each. The cell pellet was incubated in blocking buffer for 15 min at room temperature and washed with PBS. For antibody treatment, the above collected pellet were re-suspended in 80 µl FACS buffer (PBS supplemented with 1% BSA and 2mM EDTA (pH 7.4) to which was added 20 µl of direct conjugated CD45 antibody (BD Biosciences, San Jose, CA, USA) and incubated at 4 °C overnight. After a wash with PBS, cell images were captured to determine the sorting efficiency.

S.1.6 *Cell fixation protocol*

Confluent cells were detached by trypsinisation and collected by centrifugation at 1500 rpm for 7 min. The cell pellet was treated with 4% Paraformaldehyde (PFA) and incubated for 20 min at room temperature. The cell solution was washed twice with PBS and collected each time by centrifugation at 1500 rpm for 10 min.

S.1.7 *Cell regrowth protocol*

The sorted cell suspension was diluted four times in PBS and cells were collected by centrifugation at 1500 rpm for 15 min. Additional wash is required to avoid other contaminations. Long-term viability test was done by culturing MCF 7 cells after sorting. The centrifuged cells were re-suspended in DMEM with 10% FBS (Himedia) and 1% Antibiotic Antimycotic solution (Himedia). The cell suspension is seeded in a tissue culture plate (Tarsons) and its growth was monitored after 24 h and 48 h.

S.1.8 *Experimental setup*

The microchannel device was fabricated in poly dimethyl siloxane (PDMS) by following standard soft lithography procedure[5]. In the fabricated device, the expanded channel section has a width of 60 µm, depth of 28 µm and length of 5 mm. The fluidic connection between syringe pumps and the device was established using polymer tubing (Fisher Scientific, USA). All the experiments were performed using 5.0 mL and 2.5 mL glass syringes (Cetoni GmbH, Germany). The flow rates of dextran and PEG were selected to be in the range 1 – 4 µl/min and 1–12 µl/min, respectively. The dextran with cells and PEG solutions are infused into the device using two separate syringe pumps (Cetoni GmbH, Germany). From the PBMC outlet, cells were drawn using another syringe pump into a glass syringe. At the CTC outlet, cells were collected into an Eppendorf tube (Eppendorf, Germany) using a PTFE tube inserted to the outlet port. The interface location and cell migration were observed and captured using an inverted microscope (Olympus IX73) coupled with a high-speed monochrome camera operating at 7000 – 10,000 fps (FASTCAM SA3 model, Photron USA, Inc.) interfaced with a PC via Photron Fastcam Viewer software. Fluorescent images were taken using a CCD camera (ProgRes CF Cool, Jenoptik, Germany) interfaced with PC via ProgRes CapturePro v2.8.8 software.

S.1.1.I Interfacial tension (IFT) measurement

S.1.1.I(a) Direct measurement by Droplet Size Analyzer (DSA 25)

The procedure used to measure IFT using the droplet size analyzer method is outlined in Fig. S1 below.

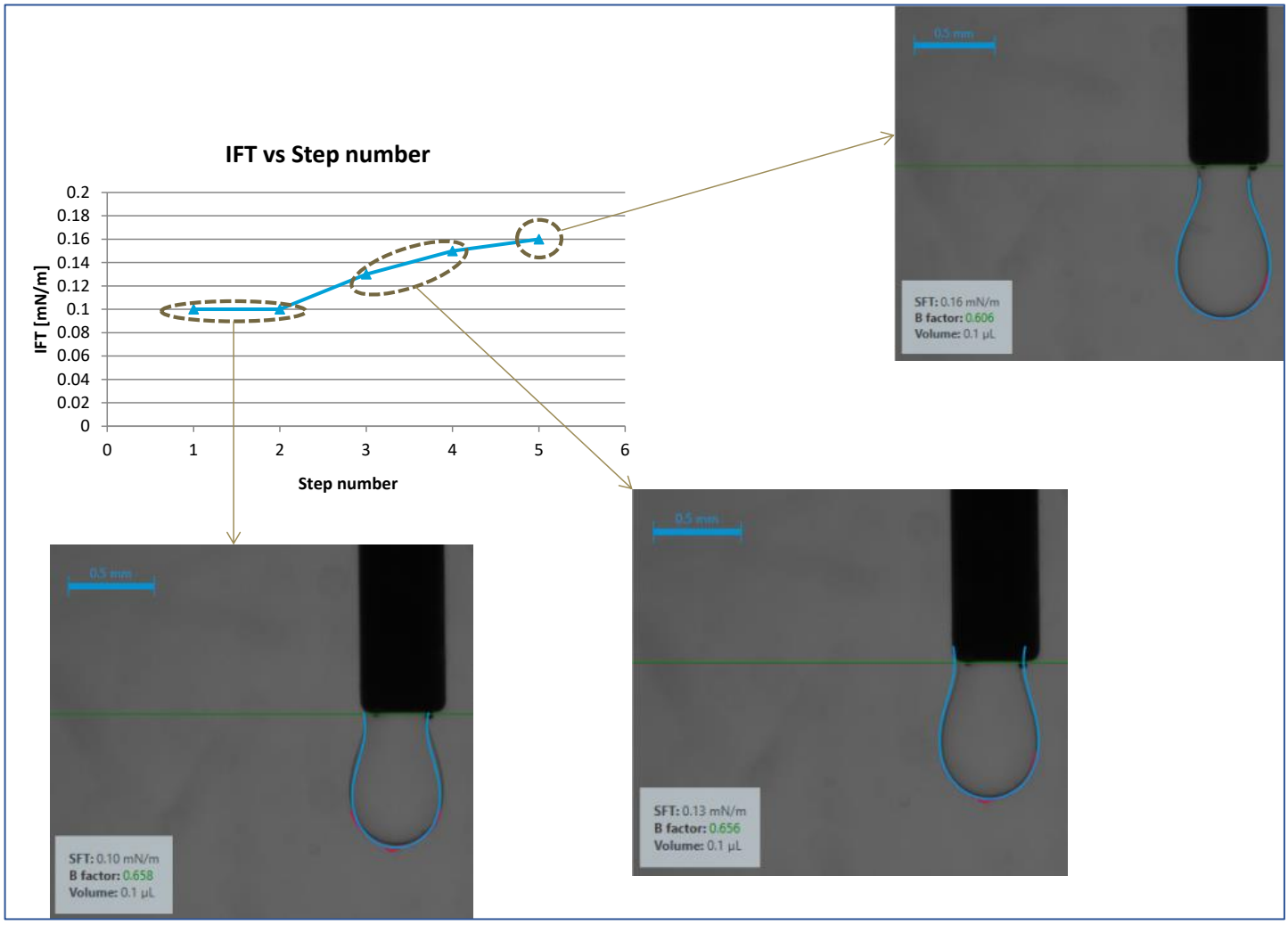

Fig. S1 IFT measurement by droplet size analyzer method.

S.1.1.I(b) Indirect Measurement (Pendant drop method)

A small volume of dextran was dispensed with a needle of diameter 0.5 mm inside PEG. Images were captured till dextran droplet completely detaches from the needle. From the image (see Fig. S2), we measured height (h) and radius of curvature(R). Using the expression available in literature (P. R. Waghmare, S. Das and S. K. Mitra, Soft Matter, 2013)[4] we determined IFT ($\gamma_{Dex-PEG}$) between Dextran and PEG as follows,

$$\gamma_{Dex-PEG} = R \times g \times h \times \frac{\rho_{dex} - \rho_{PEG}}{2} = 0.00305 \times 9.81 \times 0.0015 \times \frac{1105.3 - 1020}{2} = 0.180\, mN/m.$$

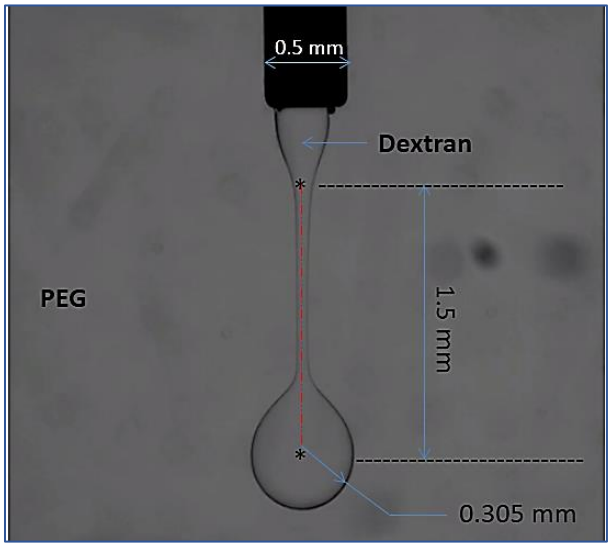

Fig. S2 IFT measurement using pendant drop method and Bernoulli's equation.

S.2 Diffusion across the interface

To determine the possibility of diffusion of both the aqueous phases across the interface, Rhodamine (Sigma-Aldrich, USA) at a volume ratio of 1:200 was added to the dextran phase and fluorescent images were captured at three different locations (i.e. at x = 0.2 mm, 2.0 mm and 5.0 mm from the junction) along the flow direction, as shown in Fig. S3(a). The normalized grey scale intensity across the channel width at the above three locations is depicted in Fig. S3(b), which shows that diffusion is negligible. We analytically calculated the self-diffusion coefficients $D_{\infty,0}$ of dextran and PEG to be 6.73×10^{-14} and 1.15×10^{-11} m^2/s, respectively, using Stokes-Einstein equation and values of the relevant parameters reported in literature[6]. Solute radius was taken to be 3 nm and 12 nm for PEG and Dextran respectively. Peclet number $Pe = \left(UD_h/D_{\infty,0}\right)$, where U is the corresponding phase velocity and D_h is the hydraulic diameter of the respective phases, was found to be very high $\sim 6 \times 10^5$. Hence, we conclude that diffusion across the interface is negligible.

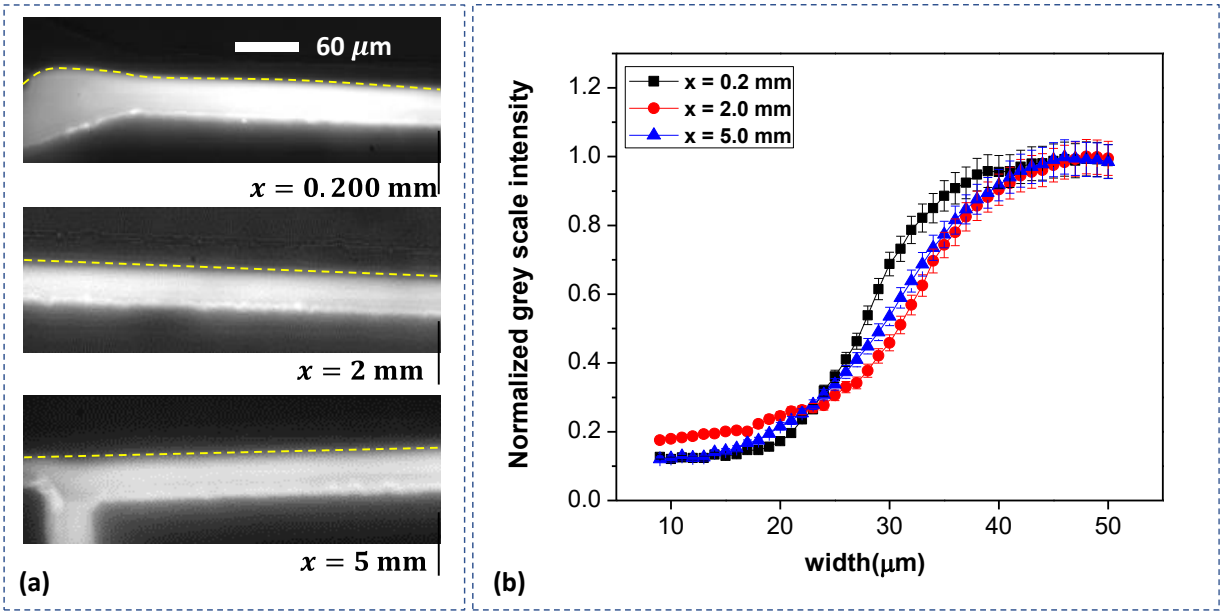

Fig. S3 Fluorescent images of ATPS with Rhodamine (at 1:200 volume ratio) added to the dextran phase, (b) Normalized grey scale intensity across the channel width at different locations ($x = 0.2, 2$ and 5 mm) in the flow direction, flowrate of dextran and PEG 1.0 and 3.0 µl/min, respectively.

S.3 Rheometry

Rheometry was performed with Anton Paar stress-controlled rheometers MCR 301 and 502. Both being rotational rheometers, cone and plate geometry was used for experiments. Cones with angle 1^0 and diameters of 25 mm and 50 mm were used. RheoPlus and RheoCompass software were used for giving input and generating raw data. All experiments were done at 25 ^{0}C. Steady shear test (Fig. S4 and S5) was done to observe dependence of viscosity on strain rate. Dextran 26% (Fig. S4) and PEG 10 % (Fig. S5) showed steady value while Dextran 30% (Fig. S4) showed shear thinning behavior.

Oscillatory shear test (Fig. S6 and S7) was done to observe possible cross over between storage and loss moduli which could lead us to define relaxation time (λ). PEG 10% (Fig. S6) and Dextran 26% (Fig. S7) showed dominant loss modulus and no cross over was observed within working range of frequency. Dextran 30% (Fig. S7) showed more prominent elastic behavior but no cross-over between storage and loss moduli was observed. From experiment it appears that in all cases, the cross over frequency is very high and relaxation time would be very low.

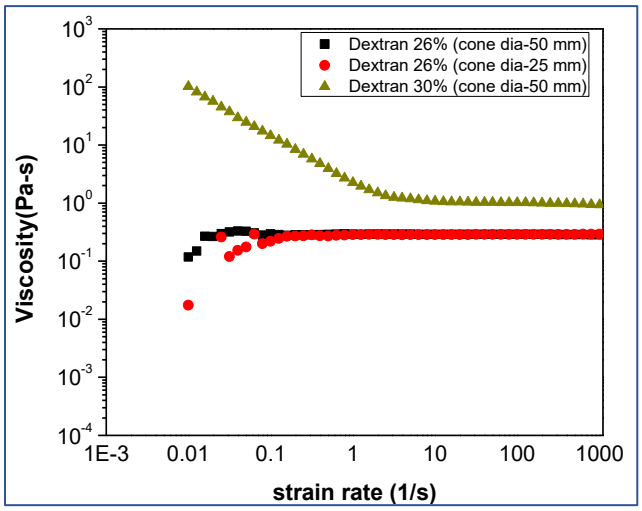

Fig. S4 Viscosity vs strain rate plots of Dextran 26 w/w % and 30 w/w % for cone diameters 25 and 50 mm.

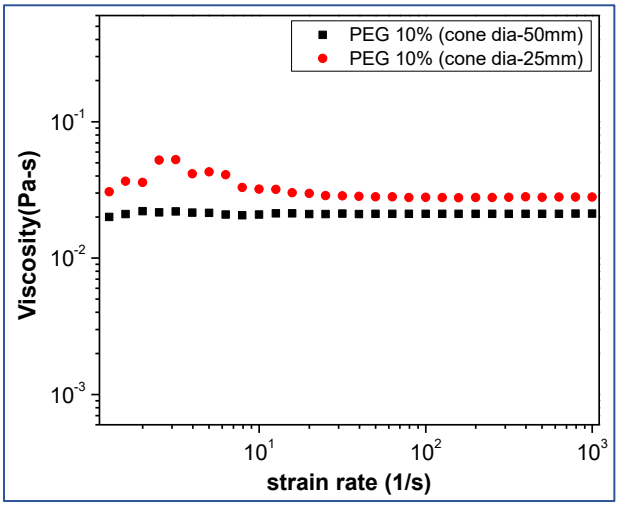

Fig. S5 viscosity vs strain rate plots of PEG 10 w/w % for cone diameters 25 and 50 mm.

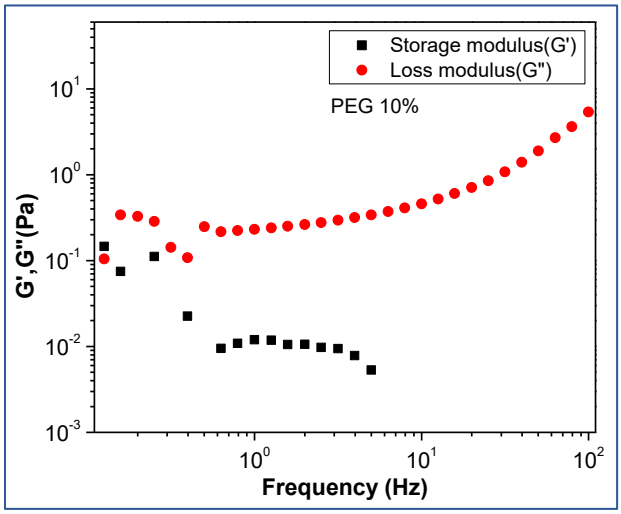

Fig. S6 Oscillatory shear test for PEG 10 w/w %. Cone diameter 50 mm.

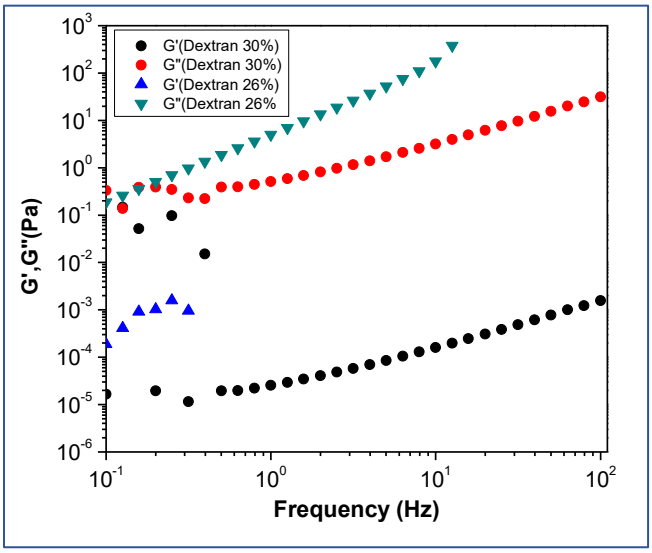

Fig. S7 Oscillatory shear test for Dextran 26 w/w % and 30 w/w %. Cone diameter 50 mm.

S.4 Simulation results for velocity profile and strain rate at different flowrates

The velocity profile at a dextran and PEG flow rate of 3 and 9 µl/min respectively is shown below (see Fig. S8).

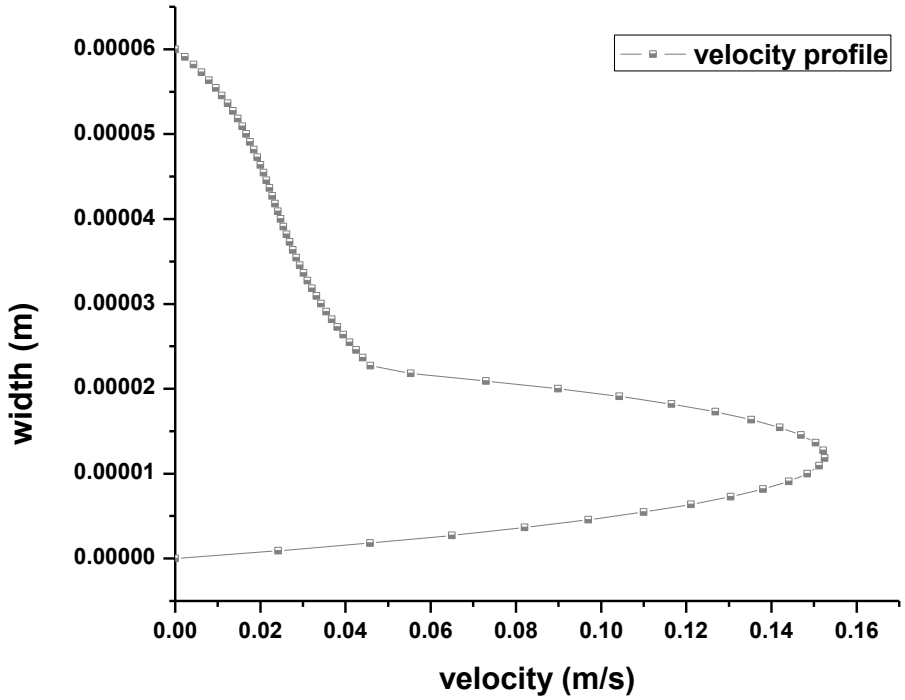

Fig. S8 Velocity profile for Dextran and PEG flowrate of 3 and 9 µl/min.

Non-inertial lift (F_l) scales as $\sim \frac{\mu\gamma R^3}{h}$. F_l, for present case is presented in Table S1. Here, μ = viscosity area averaged on x plane, γ = strain rate area averaged on x plane and h = distance of the geometric center of the cell from wall = distance of interface from wall $-$ radius of the cell

From the table it can be seen that force magnitude suddenly drops from 132.3 to 126.24 nN as flowrate changes from 3 and 9 to 4.5 and 7.5 µl/min despite the increase in strain rate. Hence 3 µl/min and 9 µl/min is taken as the optimum flowrate. At this flowrate, our device was able to perform for 4 h. Flowrate combination of 4 and 12 µl/min was not chosen due to the following reasons: (a)The flowrate yielding critical flowrate parameter ($\dot{\gamma}/h$) for PBMCs were found to be 3 and 5 µl/min. Optimum flowrate comes closer to that. It could be the best option for efficient sorting. (b) As the flowrate of Dextran is increased from 3 to 4 µl/min, the residence time of cells at the interface also decreases. (c) Operating high viscous Dextran at higher flowrate caused device failure.

Table S1: Strain data obtained from simulations.

Flow rates	Flow rate ratio	$h(\mu m)$	μ (Pa-s)	$\dot{\gamma}$ (1/s)	$\frac{\dot{\gamma}}{h}(\times 10^6)$	F_l(nN)~(For 20 μm cells)
Dex1&PEG3	0.33	27	0.181	6481.1885	240	43.23
Dex1&PEG5	0.20	23	0.163	9519.8262	413.9	67.4
Dex3&PEG5	0.60	32	0.203	13348.713	417.14	84.7
Dex3&PEG9	0.33	27	0.182	19622.393	726	132.3
Dex4.5&PEG7.5	0.60	32	0.202	19972.51	624	126.24
Dex4&PEG12	0.33	27	0.182	26143.00	968	175.8

S.5 Lift induced lateral migration of cancer cell

Fig. S9 clearly demonstrates the non-inertial lift induced lateral migration of cancer cell. A cell in Dextran phase, initially present near the wall at the beginning of the channel, can reach the interface due to the force and eventually migrate to PEG phase.

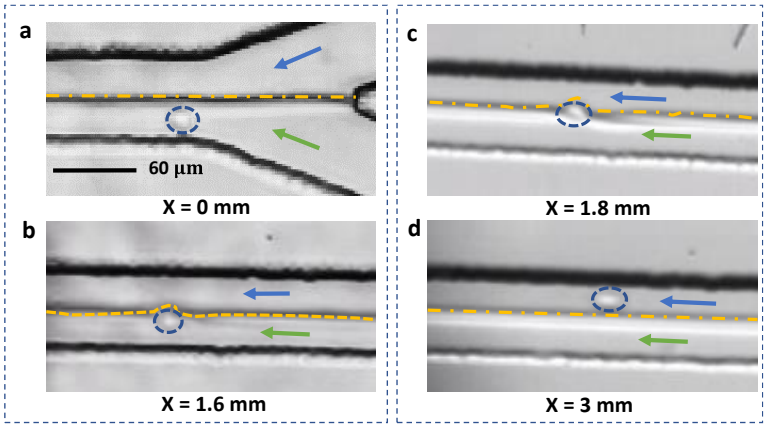

Fig. S9 a cell in Dextran starts near the wall (a) and gradually migrates to the interface (b), deforms at the interface (c) and finally migrates to PEG (d). Flowrate of dextran and PEG are 3 and 8µl/min, respectively.

S.6 Micro-Constriction Experiment

To determine Young's modulus of PBMC and MCF-7, micro-constriction experiment was carried out. Fig. S10 shows cells passing through the constriction at different time instants. The steady state velocity of MDA-MB-231, MCF-7 and PBMC of varying sizes through micro-constriction is shown in Fig. S11. The variation of extension ratio with non-dimensional cell diameter for the different cell lines are shown in Fig. S12. Size ratio is the ratio of undeformed cell diameter to the hydraulic diameter of the micro-constriction. Fig. S13 represents Young's modulus of all three cell lines.

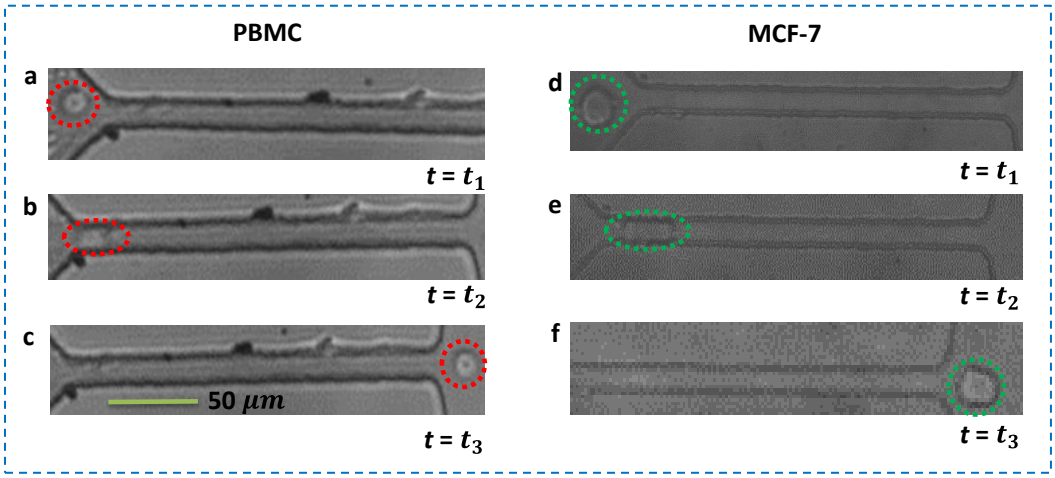

Fig. S10 Micro-constriction experiments with PBMC and MCF-7 at different time instants. Cells are undeformed before entry ($t = t_1$). Once entered, they squeeze past the constriction and deform greatly ($t = t_2$). They again attain original shape after exit ($t = t_3$).

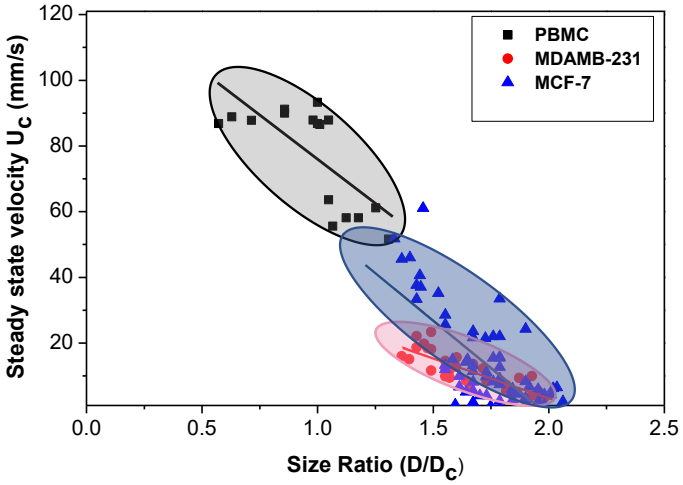

Fig. S11 Steady state velocity vs size ratio plot for MDAMB-231, MCF-7(n=30) and PBMC (n=20). MDAMB-231 data reproduced[7].

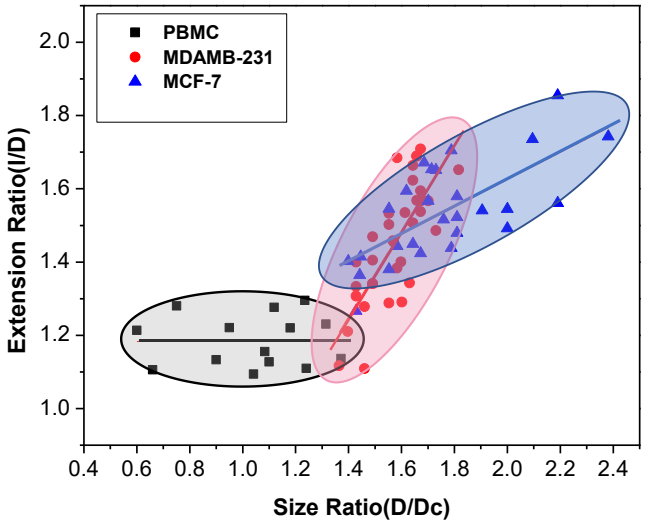

Fig. S12 Extension ratio vs size ratio plot for MDAMB-231, MCF-7(n=30) and PBMC (n=20). MDAMB-231 data was reproduced from the original paper[7].

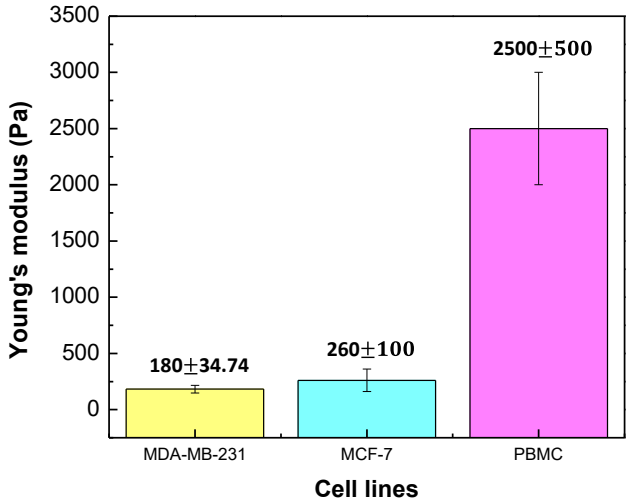

Fig. S13 Young's moduli of different cell lines used for experiment, determined following the technique developed by our group[7]. Values for MCF-7 and PBMC were calculated for present work and MDA-MB-231 data was taken from the original paper.

S.7 Schemes used for the sorting of cancer cells from PBMCs:

Using the same microchannel device (Fig. 1a), two different schemes are employed (see Fig. S14 below). In scheme A, sorting of cells takes place at a T junction while the same happens at a Y junction in scheme B. One can see that compared to scheme A, in scheme B, the flow direction is simply reversed, which should not affect the performance since we are operating in the Stokes regime.

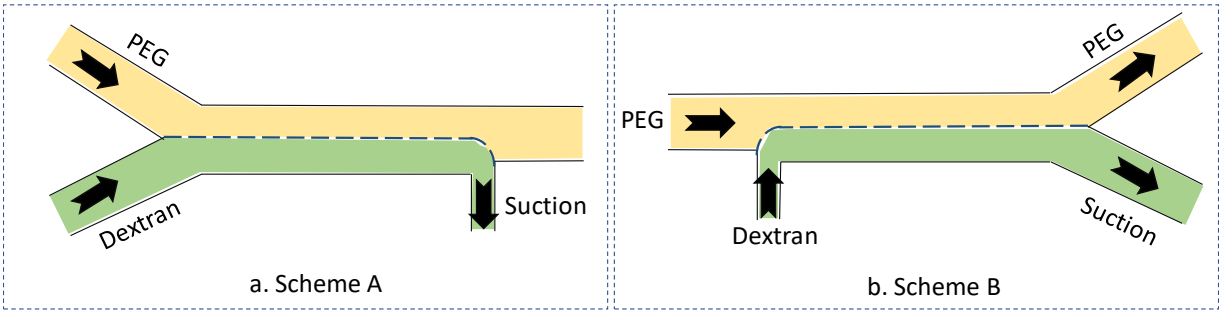

Fig. S14 Two different schemes used for the sorting of CTCs from PBMCs.

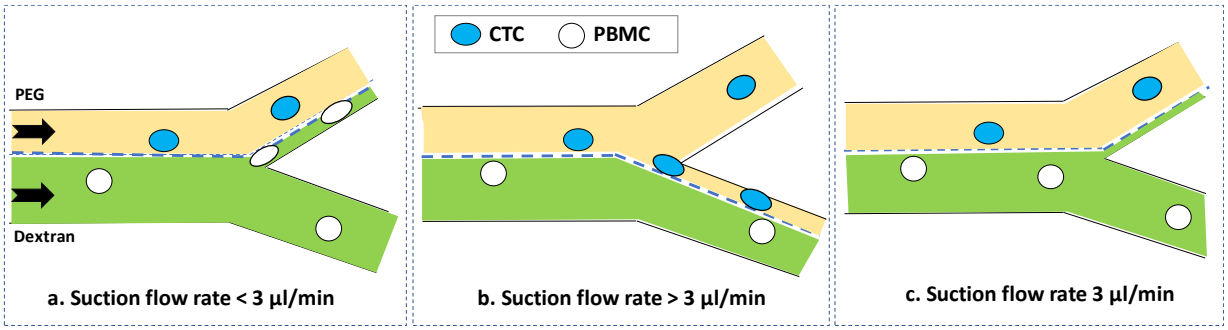

Fig. S15 (a-c) Movement of cells affected by suction flow rate of the Dextran phase.

References

(1) Ryden, J.; Albertsson, P. ake. Interfacial Tension of Dextran-Polyethylene Glycol-Water Two-Phase Systems. *J. Colloid Interface Sci.* **1971**, *37* (1), 219–222.

(2) Liu, Y.; Lipowsky, R.; Dimova, R. Concentration Dependence of the Interfacial Tension for Aqueous Two-Phase Polymer Solutions of Dextran and Polyethylene Glycol. *Langmuir* **2012**, *28* (8), 3831–3839.

(3) Forciniti, D.; Hall, C. K.; Kula, M. R. Interfacial Tension of Polyethyleneglycol-Dextran-Water Systems: Influence of Temperature and Polymer Molecular Weight. *J. Biotechnol.* **1990**, *16*, 279–296.

(4) Waghmare, P. R.; Das, S.; Mitra, S. K. Drop Deposition on Under-Liquid Low Energy Surfaces. *Soft Matter* **2013**, *9* (31), 7437.

(5) Sajeesh, P.; Doble, M.; Sen, A. K. Hydrodynamic Resistance and Mobility of Deformable Objects in Microfluidic Channels. *Biomicrofluidics* **2014**, *8* (5), 054112.

(6) Shao, J. H.; Baltus, R. E. Effect of Solute Concentration on Hindered Diffusion in Porous Membranes. *Aiche J.* **2000**, *46* (7), 1307–1316.

(7) Raj, A.; Dixit, M.; Doble, M.; Sen, A. A Combined Experimental and Theoretical Approach towards Mechano-Phenotyping of Biological Cells Using a Constricted Microchannel. *Lab Chip* **2017**, *17*, 3704–3716.